Acetylcholinesterase Staining in Human Auditory and Language Cortices: Regional Variation of Structural Features

Jeffrey J. Hutsler and Michael S. Gazzaniga

Center for Neuroscience, University of California, Davis California 95616

Cholinergic innervation of the cerebral neocortex arises from the basal forebrain and projects to all cortical regions. Acetylcholinesterase (AChE), the enzyme responsible for deactivating acetylcholine, is found within both cholinergic axons arising from the basal forebrain and a subgroup of pyramidal cells in layers III and V of the cerebral cortex. This pattern of staining varies with cortical location and may contribute uniquely to cortical microcircuitry within functionally distinct regions. To explore this issue further, we examined the pattern of AChE staining within auditory, auditory association, and putative language regions of whole, postmortem human brains.

The density and distribution of acetylcholine-containing axons and pyramidal cells vary systematically as a function of auditory processing level. Within primary auditory regions AChE-containing axons are dense and pyramidal cells are largely absent. Adjacent cortical regions show a decrease in the density of AChE-containing axons and an increase in AChE-containing pyramidal cells. The posterior auditory and language regions contain a relatively high density of AChE-containing pyramidal cells and AChE-containing axons. Although right and left posterior temporal regions are functionally asymmetrical, there is no apparent asymmetry in the general pattern of AChE staining between homologous regions of the two hemispheres. Thus, the pattern of AChE staining covaries with processing level in the hierarchy of auditory cortical regions, but does not vary between the functionally distinct right and left posterior regions.

An asymmetry in the size of layer III AChE-rich pyramidal cells was present within a number of cortical regions. Large AChE-rich pyramidal cells of layer III were consistently greater in size in the left hemisphere as compared to the right. Asymmetry in layer III pyramidal cell size was not restricted to language-associated regions, and could potentially have a variety of etiologies including structural, connectional, and activational differences between the left and right hemisphere.

Cholinergic innervation of the cortex arises from the basal forebrain and projects widely throughout the cerebral mantle (Mesulam and Geula, 1988a). This projection is thought to modulate activity within the cerebral cortex and has been implicated in such diverse cognitive tasks as learning and memory (Dunnett and Fibiger, 1993; Nabeshima, 1993), as well as attention and arousal (Muir et al., 1993). The early and dramatic reduction of cholinergic basal forebrain projections in Alzheimer's disease (Geula and Mesulam, 1989) has attracted a great deal of attention to this ubiquitous cortical system.

Cholinergic innervation of the cerebral cortex is not uniform and is known to vary between cortical regions. This variation has previously been demonstrated by examining the distribution of acetylcholinesterase (AChE), which is found in both axons and pyramidal cells in the human cortex. AChE is known to participate in cholinergic transmission by enzymatic degradation of acetylcholine that has been released for synaptic transmission (Schwartz, 1991). This is not AChE's only function within the CNS, as it has also been implicated in diverse processes such as neural differentiation, neurite extension, morphogenesis, modulation of membrane excitability, modulation of membrane permeability, and proteolysis (Silver, 1974; Greenfield, 1984, 1991; Robertson, 1987; Taylor et al., 1987; Krisst, 1989; Small, 1989, 1990). AChE-containing axons of the cerebral cortex are also immunoreactive for choline acetyltransferase (ChAT) and are therefore known to be cholinergic (Mesulam and Geula, 1992).

AChE-containing pyramidal cells of layers III and V are not cholinergic (Mesulam and Geula, 1991), but it has been suggested that they are cholinoceptive (Krnjevic and Silver, 1965; Levey et al., 1984; Mesulam et al., 1984b). In support of this notion, layer III and V pyramidal cell excitability can be modulated by the application of acetylcholine in the slice preparation (McCormick and Williamson, 1989). Additionally, muscarinic acetylcholine receptors are found on pyramidal cells of both layers III and V, as well as nonpyramidal cells (Schröder et al., 1990; Mrzljak et al., 1993). Regional variation within the cerebral cortex has been shown for both the AChE-containing axons and pyramidal cells, and it has been suggested that this variation is attributable to modifications in the processing of cortical information (Mesulam et al., 1992). Interestingly, chemical assays performed on the left and right superior temporal gyri in postmortem humans have shown higher levels of ChAT, the rate-limiting enzyme for acetylcholine production, in the left hemisphere. This difference is presumably due to the functional differences found between the left and right parietal temporal junction and their diverging roles in language (Amaducci et al., 1981).

Since relatively little is known about the microanatomical organization of regions associated with language functions, we were interested in (1) the intrahemispheric variation of AChE staining in primary, secondary, and associational auditory areas; and (2) whether functional differences between the hemispheres might be reflected in the structural and chemical organization of these regions.

Materials and Methods

Tissue Specimens

Six, whole adult human brains ranging in age from 42 to 97 years were collected at autopsy and postfixed in 4% phosphate-buffered paraformaldehyde (Tago et al., 1986; Mesulam and Geula, 1991). The time from death to fixation varied between 5 and 72 hr (see Table 1). None of the cases had any neurological or psychiatric conditions, except case 93-008 (97 years old), who had a minor cerebral vascular accident several years prior to the time of death that was not visible from gross examination of the brain. Information regarding the laterality of language functions was unavailable for this sample of brains; however, in the general population 90–95% are left hemisphere dominant for language functions as assessed by aphasia following stroke and intracarotid injections of sodium amytal (Milner, 1974; Hécaen et al., 1981). Correlates of language lateralization include hemispheric differences in the course of the sylvian fissure (Ratcliffe et al., 1980; but see Strauss et al., 1985), perceived hemispheric differences in the size of the planum temporale (Witelson, 1983; Strauss et al., 1985), and the handedness of subjects (Milner, 1974). Handedness information was not universally available for these specimens; however, each brain showed the typical pattern of a right rising sylvian fissure and

Table 1
Whole brain tissue samples

Brain	Age	Sex	Postmortem interval
93-006	50	F	72 hr to fixation
93-008	97	M	7 hr 45 min to ice 32 hr to fixation
93-010	32	F	15 hr 45 min to ice 56 hr to fixation
93-011	45	M	14 hr to fixation
93-012	58	F	10 hr to fixation
93-012	66	F	5 hr 55 min to fixation

the associated foreshortened right planum temporale (see Loftus et al., 1993).

Tissue for these studies was supplied by the National Disease Research Interchange, by Dr. Robert Ellis of the University of California Davis Medical Center, and by Dr. Robert Rafal of the Martinez Veteran's Hospital. All procedures for tissue collection were approved by the Human Subjects Committee of the University of California, Davis.

Tissue Processing

Following 48 hr of postfixation, 2 cm blocks were removed from several locations along the superior temporal gyrus, the dorsal plane of the temporal lobe, and the posterior parietal-temporal junction. Blocks were taken from a total of seven cortical locations within each hemisphere: HG (Heschl's gyrus/primary auditory cortex), ST1p (the most anterior portion of the superior temporal gyrus just behind the transverse temporal sulcus; arrow in Fig. 1*A*), ST20p (superior temporal sulcus 20 mm posterior to the transverse temporal sulcus), ST30p (superior temporal sulcus 30 mm posterior to the transverse temporal sulcus), PTa (anterior planum temporale just posterior to the transverse temporal sulcus), PTp (posterior planum temporale 30 mm posterior from the transverse temporal sulcus), and SMG (area 40; the upper bank of the supramarginal gyrus rostral to the termination the sylvian fissure). Blocks were postfixed for an additional 48 hr, embedded in agar, and cut at 50 μm on a vibratome. Every fourth section was used for acetylcholinesterase histochemistry and adjacent sections were stained for Nissl substance with thionin.

Nissl sections were used to confirm the architectonic location of morphologically selected tissue blocks. Our area HG, taken from the crown of Heschl's gyrus, showed features typical of koniocortex (Braak, 1978; Galaburda and Sanides, 1980; Ong and Garey, 1990) or Brodmann's area 41. The most anterior block taken from the superior temporal gyrus (ST1p) corresponded architectonically to the central portion of the magnopyramidal regions of Braak (1978) or area TB of von Economo (von Economo and Koskinas, 1925), while the two posterior regions ST20p and ST30p corresponded to posterior marginal zones of this same region (Braak, 1978), or in the nomenclature of Brodmann the posterior portion of area 22. In other nomenclature, area ST30p has been called area Tpt (Galaburda and Sanides, 1980), which is a subregion of von Economo's area TA_1 (von Economo and Koskinas, 1925). Cytoarchitectonic evaluation of anterior and posterior blocks taken from the dorsal surface of the temporal lobe within the planum temporale (PTa and PTp) corresponded to medial portions of Brodmann's area 42 and 22, respectively. Finally, our most posterior block taken from the supramarginal gyrus (SMG) was architectonically synonymous with Brodmann's area 40 and von Economo's area PFcm.

Acetylcholinesterase Staining

Acetylcholinesterase staining was carried out according to the methods of Karnovsky and Roots (1964) with the modification described by Tago et al. (1986). Briefly, tissue sections were rinsed in phosphate buffer for 30 min and then preincubated for 30 min in 3.4 mg tetraisopropyl pyrophosphoramide in 500 ml phosphate buffer (pH 7.4) to reduce nonspecific cholinesterase staining. Sections were then transferred to a solution containing 482.5 ml phosphate buffer, 3.4 mg tetraisopropyl pyrophosphoramide, 50 mg acetylthiocholine iodide, 294 mg sodium citrate, 75 mg cupric sulfate, 16 mg potassium ferricyanide, and 17.5 ml dH_2O (pH 5.9) for 4–8 hr. Following three 10 min rinses in Tris buffer (pH 7.2) the sections were transferred to a solution containing 50 mg 3,3′-diaminobenzidine (Sigma Chemicals), 3 ml of 0.3% H_2O_2, and 10 ml of 1% cobalt chloride. Sections were again rinsed in Tris buffer and mounted onto gelatin-coated slides. After air drying the sections were dehydrated in a graded series of ethanol, cleared in two 10 min xylene rinses, and coverslipped with Permount (Fisher Scientific).

Controls

Several control experiments were conducted to determine if our labeling was specific for acetylcholinesterase: (1) elimination of the acetylthiocholine iodide, (2) substitution of butyrylthiocholine iodide for acetylthiocholine iodide, and (3) addition of the specific AChE inhibitor 1,5-bis(4-allyldimethylammonium-phenyl)pentan-3-one. In addition, to eliminate nonspecific cholinesterase staining, tetraisopropyl pyrophosphoramide was added to the initial rinse as well as the staining substrate.

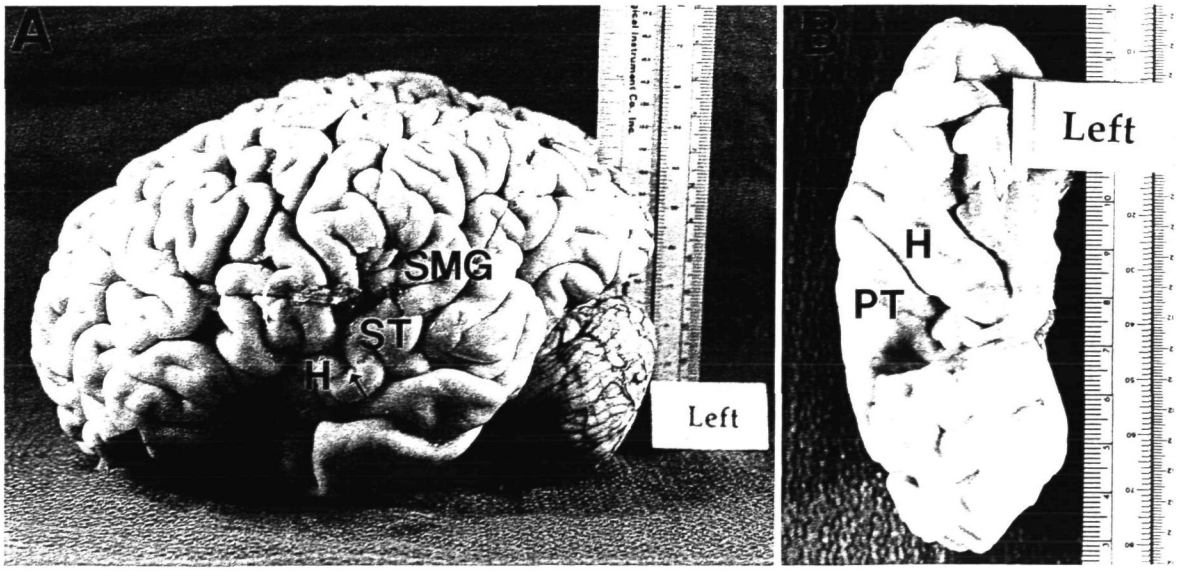

Figure 1. Photographs showing the location of regions sampled from the dorsal surface of the temporal lobes and the temporal-parietal junction. *A*, Lateral surface of the left hemisphere. *Arrow* indicates the lateral portion of the transverse temporal gyrus. *B*, Dorsal surface of the temporal lobes. *H*, Heschl's gyrus; *ST*, superior temporal gyrus; *PT*, planum temporale; *SMG*, supramarginal gyrus.

Data Analysis

Cell counts and densities were carried out on three well-stained brains in layers III and V of each cortical region examined. Only those cells that were AChE-rich as defined by Mesulam and Geula (1991)—a dark reaction product with some proximal dendrites visible—were included in the analysis (see Fig. 3). Cell densities were counted within 1 × 0.5 mm rectangles. In the case of layer III cells, the bottom, long axis of this rectangle was aligned with the border between layers III and IV. For counts made from layer V the top border of the same counting area was aligned with the border between layers IV and V. For each block of tissue, counts were made at 3 mm intervals in four sections and recorded onto enlarged drawings of the tissue sections. Subsequent analyses were performed on those counts that were well within the cytoarchitectonically defined region of interest as determined by the adjacent Nissl-stained sections. Counting boxes were positioned over regions of cortex that did not exhibit deformations associated with cortical anguli or fundi. The densities reported here represent the mean number of cells found within the counting grids located within the region of interest.

Cell sizes were measured within two sections taken from each region of four brains. In the case of layer III pyramidal cells, measurements were made within 2 linear millimeters of cortex. Layer V cells were measured from two sections within 12 linear millimeters of cortex. Individual cell somas were traced at a magnification of 500× with a camera lucida drawing tube positioned over a digitizing tablet (Kurta). Digitized tracings were collected by a Macintosh Plus computer running NIH MACMEASURE. Cell sizes for three of the four brains used in this analysis were made blind, with the experimenter having no knowledge of either the hemisphere or the region being analyzed.

Results

We will first describe the general pattern of AChE staining seen throughout the auditory and auditory association areas of both the left and right hemispheres. We will additionally describe how the density and distribution of AChE-containing axons and AChE-rich pyramidal cells varies between cortical regions and between hemispheres. Finally, we will describe the regional and hemispheric variation in AChE-containing pyramidal cell structure.

Control experiments indicated that our labeling was specific for AChE. This was demonstrated by an absence of staining following (1) the elimination of acetylthiocholine iodide, (2) the substitution of the cholinesterase butyrylthiocholine iodide, and (3) the addition of the specific AChE inhibitor 1,5-bis(4-allyldimethylammonium-phenyl)pentan-3-one. In all incubations nonspecific cholinesterase staining was inhibited with the addition of tetraisopropyl pyrophosphoramide.

General AChE Staining Pattern

AChE labels fibers throughout the extent of the cortical layers. These fibers are most dense in the upper layers, but are also prominent within layers V and VI. Fiber density is typically highest within layer II and gradually decreases from the upper to the lower strata of layer III. Layer IV, in contrast, contains a relatively low density of fibers although processes are seen transversing the layer. Layers II and III contain a preponderance of horizontal fibers, while the less dense fibers of layers V and VI are oriented horizontally, obliquely, and vertically (see Fig. 2).

AChE-containing pyramidal cells are typically found in the lower half of layer III within almost every region of cortex. The density of these cells varies considerably between regions and proximal dendrites can often be identified (see Fig. 3). Layer V also contains a number of AChE-rich pyramidal cells; however, the density of these cells is always considerably lower.

Regional Specializations

Cortical regions show a number of variations from this general pattern. Heschl's gyrus, the presumed location of primary auditory cortex, deviates significantly from this general organizational scheme. Fibers within this region are densest within layer II, and like the primary visual cortex (Mesulam and Geula, 1991), AChE-containing pyramidal cells are markedly absent from this region (see Fig. 5A). If this absence of AChE-containing cells is used to define the border between the

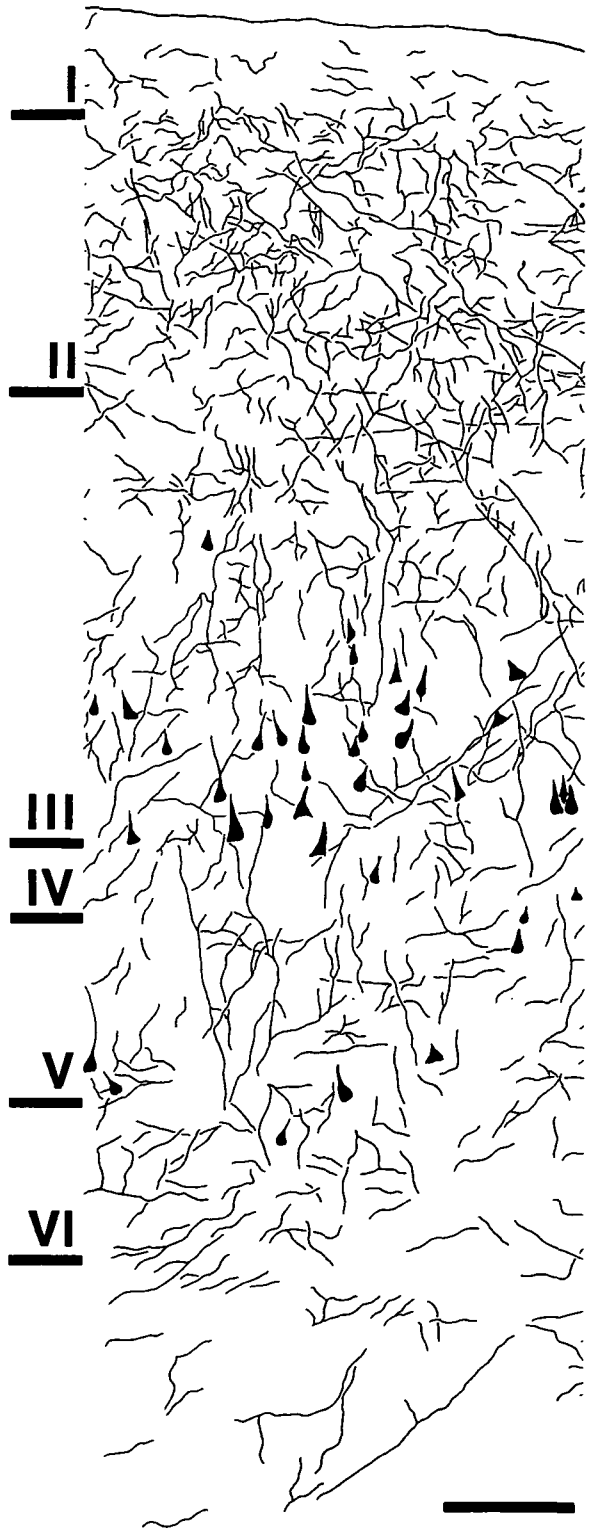

Figure 2. Camera lucida drawing of the pattern of AChE staining seen in the posterior planum temporale. AChE-containing pyramidal cells are densest in the lower portion of layer III, while the densest fibers are seen in layer II. Scale bar, 200 μm.

Figure 3. Photomicrograph of a layer III AChE-rich pyramidal cell showing the proximal dendritic arbors. Scale bar, 50 μm.

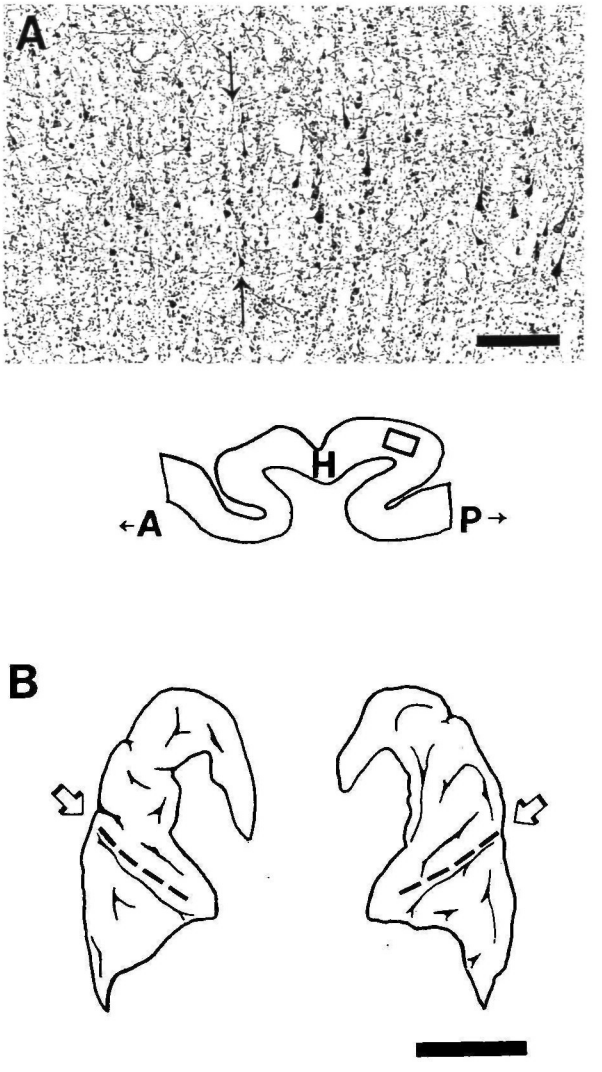

Figure 4. Location of the border between primary auditory cortex and adjacent secondary regions of case 93-013. This border typically does not coincide with the transverse temporal sulcus that is the commonly used border in studies of gross brain morphology. Secondary regions contain a number of AChE-rich pyramidal cells in layer III, while the primary auditory cortex contains few of these cells. *A*, Photomicrograph of a parasagittal section through Heschl's gyrus showing the transition zone (*arrows*) between the cell sparse region of A1 and secondary auditory cortex. *H*, Heschl's gyrus; *A*, anterior; *P*, posterior. *B*, Drawings of the dorsal surface of the right and left temporal lobes of case 93-013. *Arrows* and *dashed lines* indicate the boundary between the primary auditory region and the adjacent auditory areas as assessed by systematically examining a number of parasagittal sections through Heschl's gyrus. In both hemispheres this boundary lies anterior to the transverse temporal sulcus. Scale bars: *A*, 200 μm; *B*, 4 cm.

primary auditory region and posterior regions of the planum temporale, it is found that the posterior edge of primary auditory cortex does not coincide with the transverse temporal sulcus. The transverse sulcus is commonly utilized as the boundary between primary and secondary regions in studies of gross cortical morphology; however, the transition between AChE-cell-sparse and AChE-dense regions actually lies farther rostral and is located on the surface of the first transverse gyrus (see Fig. 4).

Of the several regions sampled from the superior temporal gyrus a gradient of effects in the staining pattern was apparent. Anterior portions of the superior temporal gyrus show a reduction in the density of fibers in the upper layer as compared to Heschl's gyrus (Fig. 5*D*). In posterior portions of the superior temporal gyrus fiber density is reduced even further within layer I (Fig. 5*E*). As with the general staining pattern described above, the densest fiber layer is always layer II, but a notable number of fibers are seen in layers III, V, and VI.

Regions sampled from the planum temporale show a high density of pyramidal cells in layer III, and a substantial number of cells are also visible in layer V. Fiber density within anterior regions of the planum are relatively high (although lower than that seen within Heschl's gyrus) and it is difficult to distinguish between layers II and III. In contrast, the posterior fiber density varies as a function of layer with a clear discontinuity between layers II and III. The distribution of cells in layer V is highly irregular through the anterior and posterior extent of the tissue giving the impression that layer V cells are found predominantly in clusters, while the distribution of AChE-rich pyramidal cells in layer III give a clear impression of a columnar arrangement (Fig. 5*C*).

Within the supramarginal gyrus the density of fibers is generally highest in layer II with a number of fibers appearing in

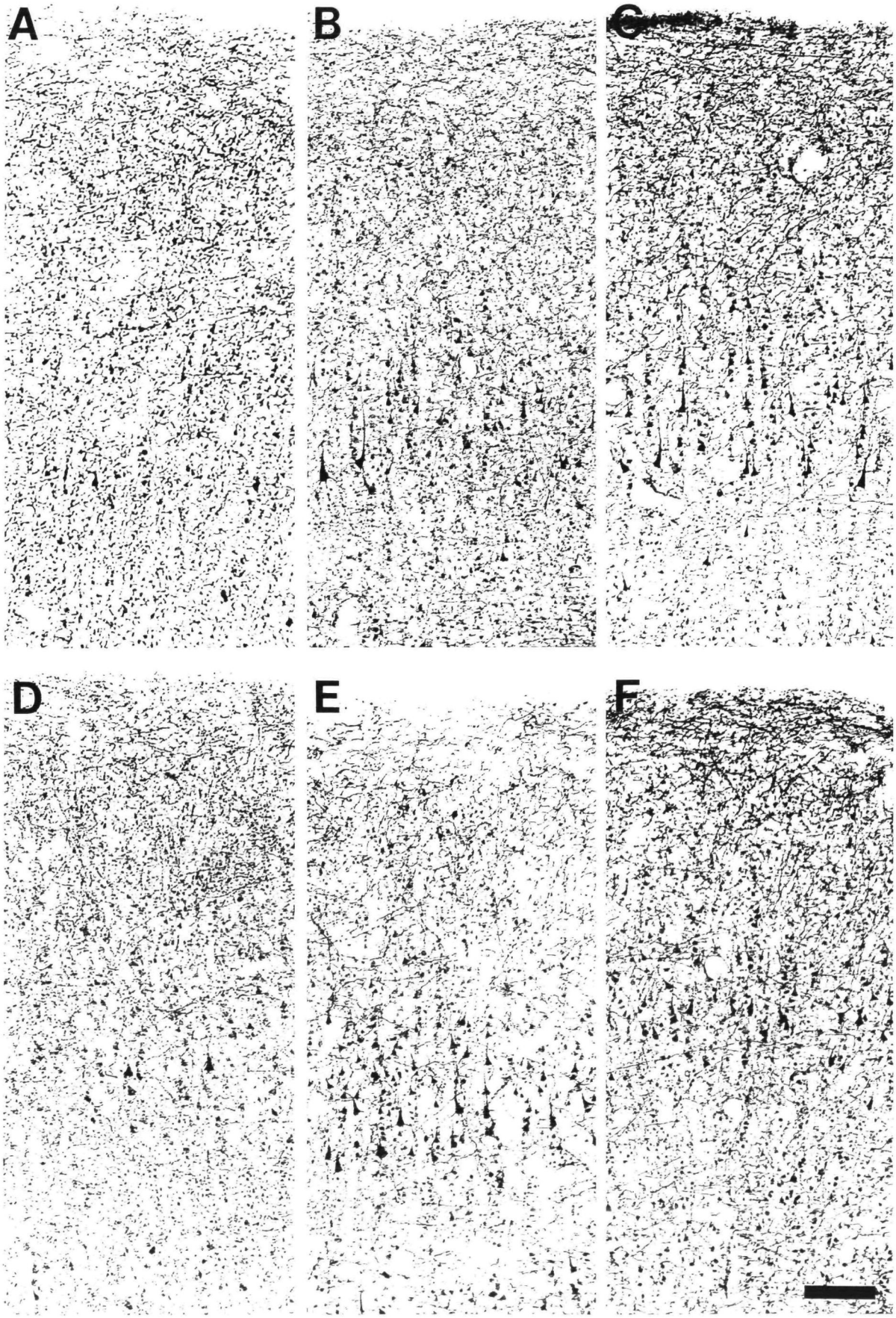

layer I. Pyramidal cells in this region are relatively dense and can often be four to five cells deep. Layer IV is clear with some tangential and horizontal fiber appearing in layers V and VI (Fig. 5*F*).

AChE-Containing Pyramidal Cell Density

Layer III pyramidal cells show a clear increase in density at increasing posterior distances from the primary auditory region. This increase occurs along both the dorsal surface of the temporal lobe and the superior temporal gyrus. Within anterior regions of the dorsal surface of the temporal lobe there are very few AChE-rich pyramidal cells in either layer III or V. The number of these cells increases systematically from the primary auditory region (Fig. 5*A*), to regions just behind the primary auditory cortex (Fig. 5*B*), to posterior regions of the planum temporale (Fig. 5*C*). Along the superior temporal gyrus the lowest density of cells is found in anterior regions (Fig. 5*D*) with a gradual increase in cell number occurring at increasingly posterior locations (Fig. 5*E*), and the highest density seen within the supramarginal gyrus (Fig. 5*F*).

The differences between primary auditory cortex (A1) and adjacent regions is clear given the near absence of AChE-containing pyramidal cells within this region. To examine the density differences outside of the primary area cell counts were made within each cortical region. The regions analyzed included three locations along the superior temporal gyrus, the anterior planum temporale, the posterior planum temporale, and the supramarginal gyrus (see Fig. 1). The mean of these layer III counts for both hemispheres from each of three brains are shown in Figure 6 (top). A repeated measures ANOVA conducted on density counts taken from six regions within both hemispheres of three brains revealed a significant difference between cortical regions ($n = 3, F = 4.922$, df = 5, $p = 0.0156$), but no density differences between hemispheres ($F = 0.433$, df = 1, $p = 0.5783$; hemisphere × region: $F = 0.738$, df = 5, $p = 0.6123$). An orthogonal set of contrasts showed density differences between anterior and posterior locations (ST1p, PTa vs ST20p, ST30p, PTp, SMG: $F = 14.882$, df = 1, $p = 0.0032$; ST20p, PTp vs ST30p, SMG: $F = 8.408$, df = 1, $p = 0.0158$), but no difference between medial and lateral regions of the dorsal plane (ST1p vs PTa: $F = 0.992$, df = 1, $p = 0.3427$; ST20p vs PTp: $F = 0.295$, df = 1, $p = 0.5986$) or the two farthest posterior locations (ST30p vs SMG: $F = 0.030$, df = 1, $p = 0.8657$). A qualitative examination of three additional brains confirmed this pattern of results.

As can be seen in Figure 6 (bottom), layer V cell densities did not vary appreciably outside of the primary auditory region. A repeated measures analysis of variance conducted on density counts from this layer confirmed that no significant differences were apparent between cortical locations or hemispheres (region: $F = 1.955$, df = 5, $p = 0.1717$; hemisphere: $F = 2.737$, df = 1, $p = 0.2398$; hemisphere × region: $F = 0.693$, df = 5, $p = 0.5787$).

Although the staining quality gives us confidence that the counts reported represent a close approximation of the number of AChE-containing pyramidal cells that are present *in vivo*, a number of factors are known to affect the outcome of cell counts, including agonal state, postmortem interval, incubation time, and the choice of fixative (but see Tago et al., 1986). Although there were some differences in the density of cells between subjects, and the aforementioned variables could contribute to the underestimation of the true cell density, we consistently found the same pattern of results in each brain analyzed (see Fig. 6): an increasing density of layer III AChE-containing pyramidal cells in posterior locations, and a lack of hemispheric asymmetry.

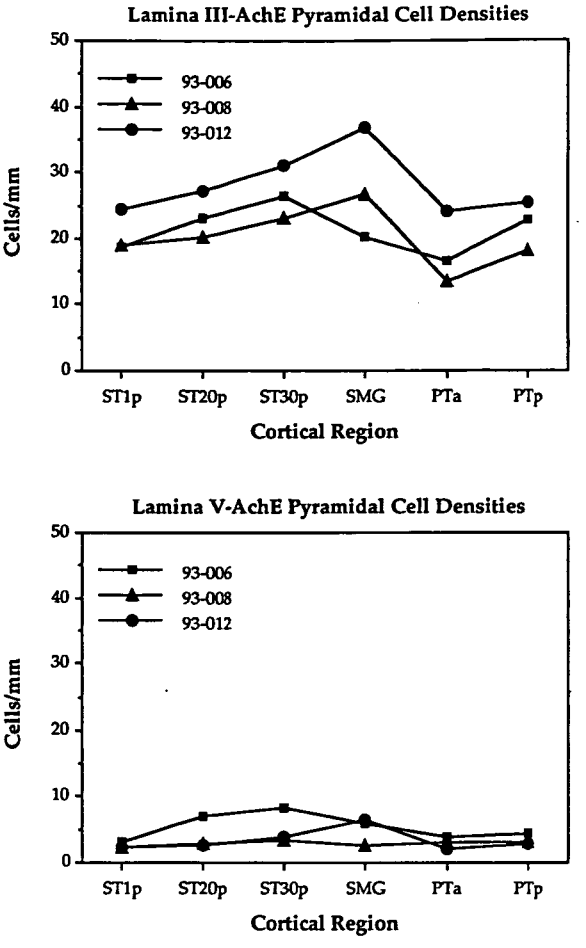

Figure 6. Density of AChE-containing cells by region for each of three cases. *Top,* Density of pyramidal cells per millimeter in layer III. *Bottom,* Density of pyramidal cells per millimeter in layer V. *ST1p,* superior temporal gyrus just posterior to the transverse temporal sulcus; *ST20p,* superior temporal gyrus 20 mm posterior to the transverse temporal sulcus; *ST30p,* superior temporal gyrus 30 mm posterior to the transverse temporal sulcus; *SMG,* supramarginal gyrus; *PTa,* anterior planum temporale; *PTp,* posterior planum temporale.

Structural Analyses

Although the variance in cell size is quite high, it was often apparent that the largest pyramidal cells within any given region differed markedly from those in the contralateral hemisphere (Fig. 7). To further explore this issue, pyramidal cell sizes were measured from seven cortical regions in each hemisphere of three brains. A comparison of cell sizes with the left and right hemispheres at comparable percentiles revealed that the largest pyramidal cells were consistently bigger in the left than the right hemisphere (Fig. 8). As we expected, given the large variance in pyramidal cell size and the restriction of this effect to only the largest subgroup of AChE-containing cells, the mean cell sizes between hemispheres

←

Figure 5. Photomicrographs showing the pattern of AChE staining and the density changes of AChE-containing pyramidal cells within each of six cortical regions. *A,* Heschl's gyrus; *B,* anterior planum temporale; *C,* posterior planum temporale; *D,* superior temporal gyrus just posterior to transverse sulcus; *E,* superior temporal gyrus, 30 mm posterior to the transverse sulcus; *F,* supramarginal gyrus. Scale bar, 200 μm.

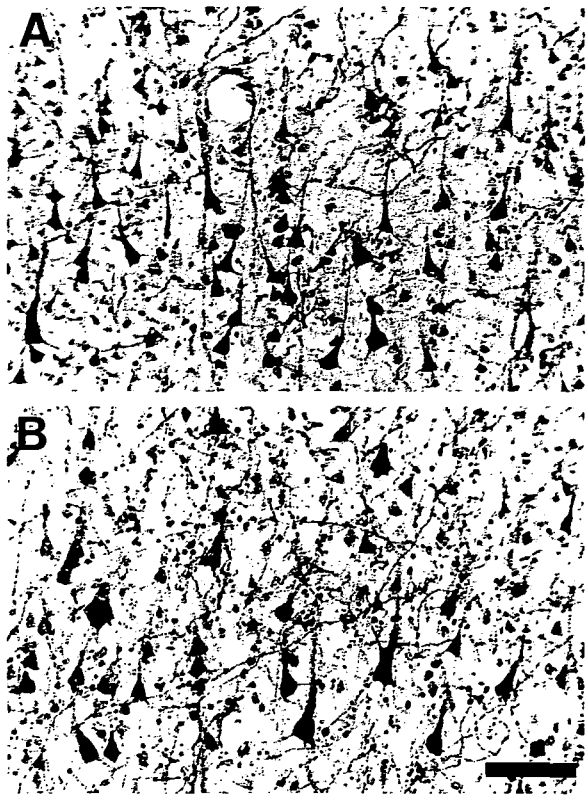

Figure 7. Photomicrographs showing the difference in cell size between the right (*A*) and left (*B*) hemispheres. Size differences are most notable when comparing the largest cells from each region. Scale bar, 100 μm.

(see Fig. 9 legend) were not significantly different. If, however, the analysis was restricted to the only the largest pyramidal cells (Hayes and Lewis, 1993), it was found that cells in the left hemisphere were significantly larger than those in the right ($F = 22.545$, df = 1, $p = 0.0416$). There were no significant size differences between regions ($F = 1.085$, df = 4, $p = 0.4250$), and no interaction of hemisphere and region ($F = 0.278$, df = 4, $p = 0.8845$).

Since it could be argued that such a restricted analysis violates the assumption of normality, a nonparametric binomial analysis was applied to the same three cases. In this analysis the largest 10% of the AChE-containing pyramidal cells sampled from each brain were examined to determine in which hemisphere these cells were more likely to be found. In all three cases, a significant proportion of the largest cells were found in the left hemisphere (Fig. 10); results for each brain are given as the number of cells in the analysis, the probability of any given cell being in the left hemisphere, the number of cells that were actually in the left hemisphere, and the normalized binomial probability [case 93-006: $N = 171$, p(left) = 0.5176, left = 106, $p = 0.0037$; case 93-012: $N = 491$, p(left) = 0.46363, left = 304, $p < 0.0001$; case 93-013: $N = 195$, p(left) = 0.5046, left = 126, $p < 0.0001$]. Since large cells are known to decrease in size with aging (Terry et al., 1987) we conducted the same analyses for the 97-year-old in our sample. In this case the difference between hemispheres was not significant. Qualitative analysis of the data indicated that overall the mean cell size in the right hemisphere (411.11 ± 8.94) was larger than that found in the left (367.32 ± 6.47 μm²). Using the same nonparametric analysis of the largest 10% of the cells measured from this brain it was found that the location of the largest cells did not differ significantly

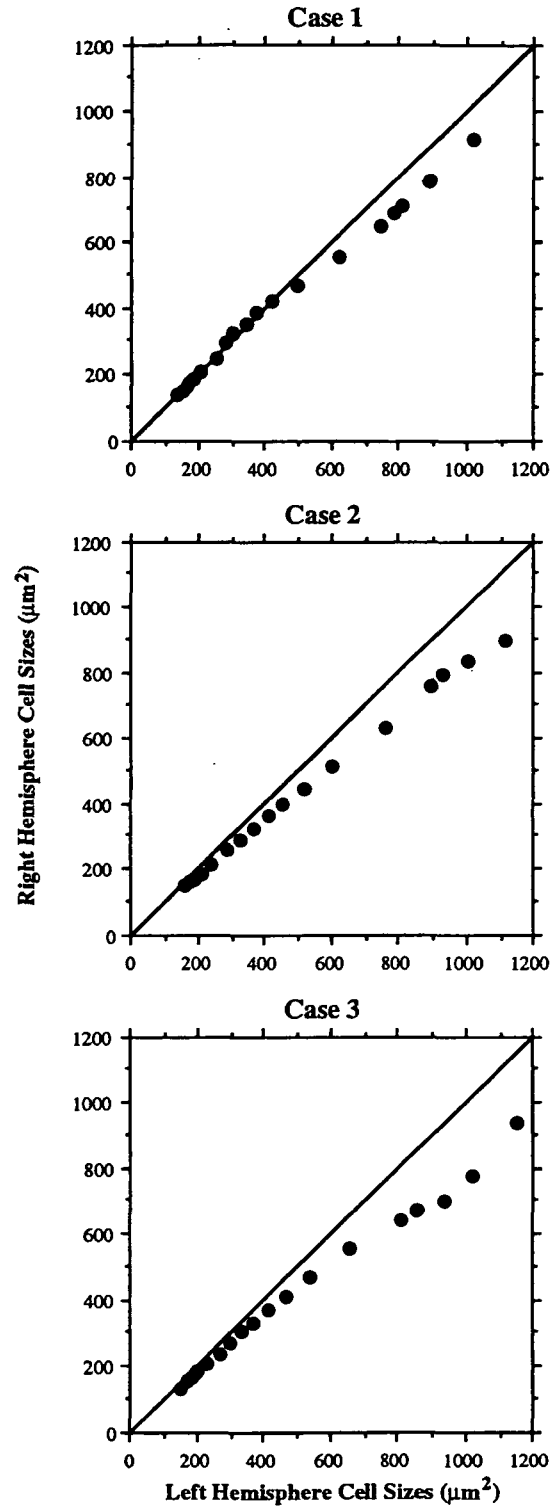

Figure 8. Comparison of cells size in the left and right hemisphere at several percentiles. In each case the difference between the left and right hemisphere increases at the higher percentiles and always shows a leftward bias. Percentiles plotted are the 1st, 2nd, 3rd, 4th, 5th, 10th, 20th, 30th, 40th, 50th, 60th, 70th, 80th, 90th, 95th, 96th, 97th, 98th, and 99th percentiles.

from chance ($N = 111$, p(left) = 0.6019, left = 65, $p = 0.82454$).

To determine whether this size asymmetry is specific to the subgroup of AChE-containing pyramidal cells or is a general property of pyramidal cells within layer III, the soma sizes

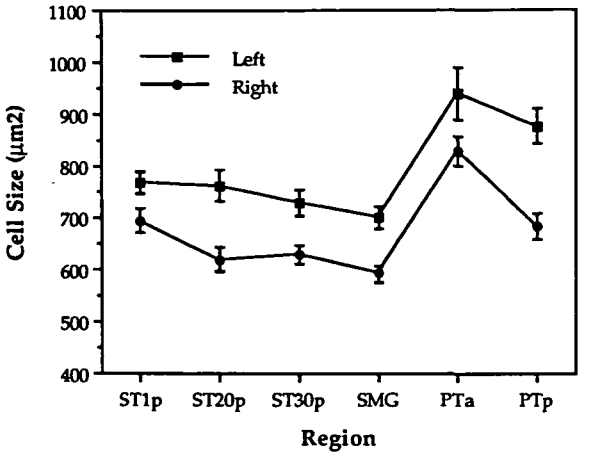

Figure 9. Pyramidal cell size and standard error as a function of regional location and hemisphere for three subjects. Each data point represents the mean of 90 cells (the 30 largest pyramidal cells for each of three subjects sampled within the region). In every region examined cells from the left hemisphere were consistently larger. The mean size of all the pyramidal cells sampled within a region was also consistently larger in the left hemisphere; however, these differences were not statistically significant (left ST1p = 462.2 μm^2 ± 8.2, n = 586; right ST1p = 399.7 μm^2 ± 8.8, n = 483; left ST20p = 475.8 μm^2 ± 12.6, n = 370; right ST20p = 380.7 μm^2 ± 7.0, n = 588; left ST30p = 388.6 μm^2 ± 7.8, n = 617; right ST30p = 363.1 μm^2 ± 5.6, n = 717; left PTa = 494.4 μm^2 ± 10.6, n = 583; right PTp = 410.1 μm^2 ± 10.0, n = 354, left PTp = 403.1 μm^2 ± 7.8, n = 782; right PTp = 403.1 μm^2 ± 7.8, n = 591).

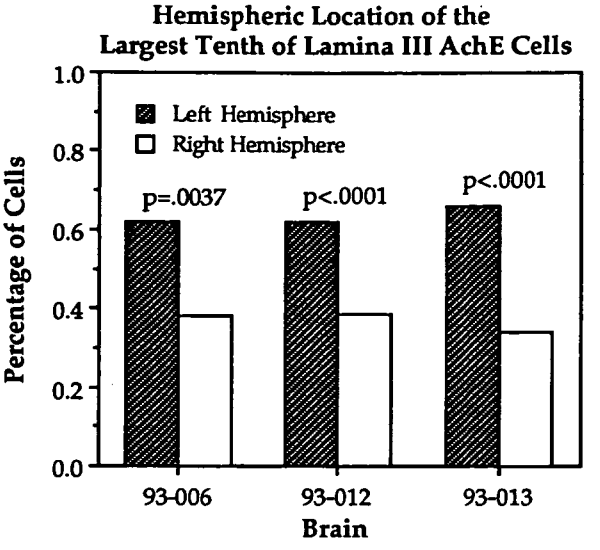

Figure 10. Hemispheric location of the largest tenth of the layer III pyramidal cells measured from each brain. The binomial probability of each result is indicated and correctly reflects the unequal sample sizes between the left and right hemisphere of each case.

of Nissl-stained pyramidal cells were measured in one brain (93-006). The mean cell size of this larger population was considerably smaller (150.83 μm^2) than the mean cell size of the AChE-containing pyramidal cells (381.87 μm^2). As with the AChE-containing pyramidal cells, Nissl cells in the left hemisphere were larger than those in the right (161.571 vs 139.68). An analysis of the largest subgroup of these cells revealed that the largest Nissl-stained cells were found predominantly in the left hemisphere. This structural asymmetry was also apparent within Heschl's gyrus (primary auditory cortex) and did not appear to be specific to regions located in the posterior parietotemporal junction (Hutsler and Gazzaniga, 1995).

Discussion

We have shown that the pattern of AChE staining within auditory and auditory association areas varies as a function of cortical location. AChE-containing axons have a high density within primary auditory regions. These processes are also dense outside of the region, but show a relatively low density in regions just adjacent to primary auditory cortex. AChE-containing pyramidal cells, while mostly absent within the primary auditory region, are found within layers III and V of every nonprimary cortical region examined. The density of these cells in layer V is low and relatively constant at various locations. In contrast, layer III pyramidal cell densities are higher overall, and increase from anterior to posterior regions. Variation in the density of AChE-containing pyramidal cells is absent between hemispheres; however, the size of the largest subgroup of these cells was found to be greater in the left hemisphere than the right. Subsequent analysis of Nissl-stained pyramidal cells in layer III indicated that this hemispheric difference was not restricted to AChE-containing pyramidal cells, or language-associated cortical regions.

Regional Variation

Regional variation in AChE-containing pyramidal cell densities systematically follows the hierarchical flow of information through cortical auditory regions. Evidence from macaque monkeys indicates that the primary auditory region is discretely located on the dorsal surface of the temporal lobe (Merzenich and Brugge, 1973; Galaburda and Pandya, 1983; Seltzer and Pandya, 1989), and that secondary auditory regions abut the posterior border of the primary auditory cortex. Furthermore, anatomical studies in this species have proposed a series of four rostrocaudal stages of information processing (Galaburda and Pandya, 1983). Anatomical tract tracing with horseradish peroxidase reveals that each field projects heavily to the adjacent region, but that connections between nonadjacent field are sparse. In humans positron emission tomography studies have localized the primary auditory cortex to Heschl's gyrus and have demonstrated that the general tonotopic organization found in monkey cortex is also present in the human auditory system (Lauter et al., 1985). Architectonic similarities between the macaque and human auditory cortex suggest that the most basic components of hierarchical organization have been partially retained in evolutionary time (Galaburda and Sanides, 1980), and functional assessment using intraoperative recording, PET, regional cerebral blood flow, and lesions studies support this view (Knopman et al., 1982; Creutzfeldt et al., 1989; Zatorre, 1992).

It is well accepted that the density of AChE-containing fibers and pyramidal cells varies between major types of cortex (Okinaka et al., 1961; Mesulam et al., 1984a; Mesulam and Geula, 1988b, 1991; Mrzljak and Goldman-Rakic, 1992). Our findings support this view, and further suggest that variation in the distribution of AChE is not dependent upon a region's functional modality as revealed through the lack of hemispheric asymmetry in the most posterior cortical locations examined. It should be noted, however, that although density does not vary between the hemispheres the total number of AChE-containing cells within an architectonically defined cortical region (total number = density × regional area) may still be asymmetrical, where hemispheric differences in the size of cortical regions exists (Galaburda et al., 1978).

An asymmetry in the level of choline acetyltransferase (ChAT), the rate limiting enzyme for acetylcholine production, has previously been demonstrated in blocks of tissue taken from the superior temporal gyri. Chemical assay of punches from these regions show increasing levels of ChAT at more posterior locations and a greater quantity of ChAT in

left cortical regions (Amaducci et al., 1981). The variation of AChE-containing fibers we find does not account for these findings; however, the relationship between axonal density and the level of ChAT is also dependent upon the number of synaptic boutons made by a single axon, the quantal size of acetylcholine release during a given action potential, and the agonal state. Additionally, the variation in the size and density of AChE-containing cells does not account for this result since cortical pyramidal cells do not contain ChAT (Mesulam et al., 1992).

Functional Implications for Cortical Circuitry

Although the presence of the appropriate degrading enzyme within cortical structures is not sufficient for the identification of cholinergic synaptic transmission, AChE has been shown to be localized in cholinergic axons (Mesulam et al., 1992). Additionally, acetylcholine modulates the excitability of human cortical pyramidal cells of layers III and V in tissue slice by reducing the potassium afterhyperpolarizing current and increasing the probability of action potential generation (McCormick and Williamson, 1989). AChE-containing pyramidal cells are a likely site of cholinergic action within the cortex, but these cells are not the only cholinoceptive neurons present within the cerebral mantle. Studies examining the distribution of muscarinic receptors in surgically resected human cortical tissue show that these receptors are located on the apical dendrites of pyramidal cells in layers II, III, and V. Other nonpyramidal cells are also labeled and these appear in layers III, IV, and VI (Schröder et al., 1990). The distribution of particular receptor subtypes—most notable the m1 and m2 receptor—has been examined in the macaque monkey (Mrzljak et al., 1993). In this species, cholinergic m1 and m2 receptors are found at both symmetric and asymmetric synapses on dendritic shafts and spines. Additionally, the m2 receptor does not appear to be an exclusively presynaptic receptor but is also found postsynaptically on both pyramidal and nonpyramidal neurons. These results indicate that acetylcholine may play an important role in modulating thalamocortical and/or corticocortical excitatory amino acid transmission.

Potential models for the contribution of cholinergic systems to the processing of auditory information are clearly dependent upon which portion of the regional variation is emphasized. The variation in cholinergic axonal fibers indicates that innervation from the basal forebrain contributes nonuniformly to cortical processing within unimodal auditory cortex and posterior association regions, but that this contribution does not vary between functionally diverse cortical regions in the left and right hemispheres. Additionally, if AChE-containing pyramidal cells represent a group of neurons that are highly responsive to cholinergic input, then it could be argued that an increasing population of cholinoceptive layer III pyramidal cells—cells that relay information to other cortical locations—results in a greater role for acetylcholine in modulating the excitability of cortical outputs in posterior regions.

Cell Size Asymmetry

Cell size differences between the left and right hemispheres have been reported by Hayes and Lewis (1993) in Nissl sections of area 45 within the frontal lobes (Broca's area). As in the present study, only the largest pyramidal cells within layer III of the left and right hemisphere showed this difference. Our findings indicate that this result is not unique to Broca's area and may not be unique to language-associated regions. The cell size differences reported here are not restricted to posterior language-associated regions, but are also found in anterior regions thought to be primarily auditory in function. We posit three interpretations that can be applied to this finding: (1) cell size differences may be related to differences in the targets of projection neurons and could, therefore, reflect a connectional difference between the hemispheres; 2) cell size differences may be a product of differing electrical activity that has previously been shown to play a role in cell size regulation (Pasic and Rubel, 1989); and (3) the asymmetry in cell size may be a portion of an already recognized asymmetry in the structural organization of the left and right hemispheres that has been reported as wider spacing between columns and longer total dendritic length of layer III pyramidal cells in the left hemisphere. Whether these large cells and longer basal dendrites result in connectional differences between the two hemispheres has not been adequately explored, although it has been suggested that the two results in combination could yield no net connectional asymmetry (Seldon, 1981a,b, 1982; Jacobs and Scheibel, 1993).

Conclusions

Structural explanations for the functional asymmetry seen between the posterior temporal-parietal regions have long been sought. Although many size asymmetries have been reported between the hemispheres (e.g., Geschwind and Levitsky, 1968; see also Witelson and Kigar, 1988, for a review), these results may be more accurately explained by differences in the folding of the cortex and methodological considerations (Loftus et al., 1993; but see Galaburda et al., 1978). Since size alone does not appear to account for language specialization within the left hemisphere, it is reasonable to ask whether specialization for language function is dependent upon the presence of specialized microcircuitry. Although relatively few studies have pursued this issue, many notable exceptions exist and these concentrate mainly on neuronal structure as assessed by Golgi impregnation (Seldon, 1981a,b, 1982; Jacobs and Scheibel, 1993; Jacobs et al., 1993).

The present study indicates that cholinergic innervation of auditory and auditory association regions in the human temporal lobes varies as a function of processing level. Additionally, despite the dramatic functional laterality seen in posterior auditory regions, the density of AChE staining varies neither for AChE-positive pyramidal cells or AChE-containing axons. AChE staining does, however, reveal a structural difference between the left and right hemisphere: a preponderance of the largest layer III pyramidal cells are found within regions of the left hemisphere. The meaning of this basic structural difference remains to be explored. Additionally, the general approach of comparing posterior temporal lobes by using neurochemical markers to examining the homologies and differences in particular portions of the cortical circuit may assist in revealing important differences between these functionally diverse regions. The lack of hemispheric asymmetry in the cholinergic subsystem may not be surprising given the widespread neuromodulatory role of acetylcholine throughout the neocortex.

Notes

We thank Dr. Robert Ellis of the University of California Medical Center, Dr. Robert Rafal of the Martinez Veteran's Hospital, and the National Disease Research Interchange for graciously providing the tissue used in this study. We also thank Dr. Leo Chalupa for his critical reading of an earlier draft of the manuscript, and Ms. Thea Ward for her technical assistance. Support for this project was provided by the McDonnell-Pew Foundation.

Address correspondence to Jeffrey J. Hutsler, Center for Neuroscience, University of California, Davis, CA 95616.

References

Amaducci L, Sorbi S, Albanese A, Gainotti G (1981) Choline acetyltransferase (ChAT) activity differs in the right and left human temporal lobes. Neurology 31:799–805.

Braak, H (1978) On magnopyramidal temporal fields in the human brain—probable morphological counterparts of Wernicke's sensory speech region. Anat Embryol (Berl) 152:141–169.
Creutzfeldt O, Ojemann G, Lettich E (1989) Neuronal activity in the human lateral temporal lobe. I. Responses to speech. Exp Brain Res 77:451–475.
Dunnett SB, Fibiger HC (1993) Role of forebrain cholinergic systems in learning and memory: relevance to the cognitive deficits of aging and Alzheimer's dementia. Prog Brain Res 98:413–420.
Galaburda AM, Pandya DN (1983) The intrinsic architectonic and connectional organization of the superior temporal region of the rhesus monkey. J Comp Neurol 221:169–184.
Galaburda A, Sanides F (1980) Cytoarchitectonic organization of the human auditory cortex. J Comp Neurol 190:597–610.
Galaburda AM, Sanides F, Geschwind N (1978) Human brain: cytoarchitectonic left-right asymmetries in the temporal speech region. Arch Neurol 35:812–817.
Geschwind N, Levitsky W (1968) Human brain: left-right asymmetries in temporal speech region. Science 162:186–187.
Geula C, Mesulam MM (1989) Cortical cholinergic fibers in aging and Alzheimer's disease: a morphometric study. Neuroscience 33: 469–481.
Greenfield SA (1984) Acetylcholinesterase may have novel function in the brain. Trends Neurosci 7:364–368.
Greenfield SA (1991) A noncholinergic action of acetylcholinesterase (AChE) in the brain: from neuronal secretion to the generation of movement. Cell Mol Neurobiol 11:55–77.
Hayes TL, Lewis DA (1993) Hemispheric differences in layer III pyramidal neurons of the anterior language area. Arch Neurol 50: 501–505.
Hécaen H, De Agostini M, Monzon-Montes A (1981) Cerebral organization in left-handers. Brain Lang 12:261–284.
Hutsler JJ, Gazzaniga MS (1995) Hemispheric differences in layer III pyramidal cell sizes—a critical evaluation of asymmetries within auditory and language cortices. Soc Neurosci Abstr 21:438.
Jacobs B, Scheibel AB (1993) A quantitative dendritic analysis of Wernicke's area in humans. I. Lifespan changes. J Comp Neurol 327:83–96.
Jacobs B, Schall M, Scheibel AB (1993) A quantitative dendritic analysis of Wernicke's area in humans. II. Gender, hemispheric, and environmental factors. J Comp Neurol 327:97–111.
Karnovsky MJ, Roots L (1964) A 'direct coloring' thiocholine method for cholinesterases. J Histochem Cytochem 12:219–221.
Knopman DS, Rubens AB, Klassen AC, Meyer MW (1982) Regional cerebral blood flow correlates of auditory processing. Arch Neurol 39:487–493.
Kristt DA (1989) Acetylcholinesterase in immature thalamic neurons: relation to afferentation, development, regulation and cellular distribution. Neuroscience 29:27–43.
Krnjevic K, Silver A (1965) A histochemical study of cholinergic fibers in the cerebral cortex. J Anat 99:711–759.
Lauter JL, Herscovitch P, Formby C, Raichle ME (1985) Tonotopic organization in human auditory cortex revealed by positron emission tomography. Hearing Res 20:199–205.
Levey AI, Wainer BH, Rye DB, Mufson EJ, Mesulam MM (1984) Choline acetyltransferase immunoreactive neurons intrinsic to rodent cortex and distinction from acetylcholinesterase-positive neurons. Neuroscience 13:341–353.
Loftus WC, Tramo MJ, Thomas CE, Green RL, Nordgren RA, Gazzaniga MS (1993) Three-dimensional quantitative analysis of hemispheric asymmetry in the human superior temporal region. Cerebral Cortex 3:348–355.
McCormick DA, Williamson A (1989) Convergence and divergence of neurotransmitter action in human cerebral cortex. Proc Natl Acad Sci USA 86:8098–8102.
Merzenich M, Brugge JF (1973) Representation of the cochlear partition on the superior temporal plane of the macaque monkey. Brain Res 50:275–296.
Mesulam M, Geula C (1988a) Nucleus basalis (Ch4) and cortical cholinergic innervation of the human brain: morphology, cytochemistry, connectivity and some behavioral implications. J Comp Neurol 275:216–240.
Mesulam M, Geula C (1988b) Acetylcholinesterase-rich neurons of the human cerebral cortex: cytoarchitectonic and ontogenetic patterns of distribution. J Comp Neurol 275:216–240.
Mesulam MM, Geula C (1991) Acetylcholinesterase-rich neurons of the human cerebral cortex: cytoarchitectonic and ontogenetic patterns of distribution. J Comp Neurol 306:193–220.
Mesulam M, Geula C (1992) Overlap between acetylcholinesterase-rich and choline acetyltransferase-positive (cholinergic) axons in human cerebral cortex. Brain Res 577:112–120.
Mesulam M, Mufson AI, Levey AI, Wainer BH (1984a) Atlas of cholinergic neurons in the forebrain and upper brainstem of the macaque based on monoclonal choline acetyltransferase immunohistochemistry and acetylcholinesterase histochemistry. Neuroscience 12:669–686.
Mesulam M, Rosene AD, Mufson EJ (1984b) Regional variations in cortical cholinergic innervation: chemoarchitectonics and acetylcholinesterase-containing fibers in the macaque brain. Brain Res 311:245–258.
Mesulam M, Hersh LB, Mash DC, Geula C (1992) Differential cholinergic innervation within functional subdivisions of the human cerebral cortex: a choline acetyltransferase study. J Comp Neurol 318:316–328.
Milner B (1974) Hemisphere specialization: scope and limits. In: The neurosciences: third study program (Schmitt FO, Worden FG, eds), pp 75–89. Cambridge, MA: MIT Press.
Mrzljak L, Goldman-Rakic PS (1992) Acetylcholinesterase reactivity in the frontal cortex of human and monkey: contribution of AChE-rich pyramidal neurons. J Comp Neurol 324:261–281.
Mrzljak L, Levey AI, Goldman-Rakic PS (1993) Association of m1 and m2 muscarinic receptor proteins with asymmetric synapses in the primate cerebral cortex: morphological evidence for cholinergic modulation of excitatory neurotransmission. Proc Natl Acad Sci USA 90:5194–5198.
Muir JL, Page KJ, Sirinathsinghji DJ, Robbins TW, Everitt BJ (1993) Excitotoxic lesions of basal forebrain cholinergic neurons: effects on learning, memory, and attention. Behav Brain Res 57:123–131.
Nabeshima T (1993) Behavioral aspects of cholinergic transmission: role of basal forebrain cholinergic system in learning and memory. Prog Brain Res 98:405–411.
Okinaka S, Yoshikawa M, Uono M, Muro T, Mozai T, Igata A, Tanabe H, Veda S, Tomonaga M (1961) Distribution of cholinesterase activity in the human cerebral cortex. Am J Phys Med 40:135–146.
Ong Y, Garey LJ (1990) Neuronal architecture of the human temporal cortex. Anat Embryol (Berl) 181:351–364.
Pasic T, Rubel EW (1989) Rapid changes in cochlear nucleus cell size following blockade of auditory nerve electrical activity in gerbils. J Comp Neurol 283:474–480.
Ratcliffe G, Dila C, Taylor L, Milner B (1980) The morphological asymmetry of the hemispheres and cerebral dominance for speech: a possible relationship. Brain Lang 11:87–98.
Robertson DA (1987) A morphogenetic role for transiently expressed acetylcholinesterase in developing thalamocortical systems? Neurosci Lett 75:259–264.
Schröder H, Zilles K, Luiten PGM, Strosberg AD (1990) Immunocytochemical visualization of muscarinic cholinoceptors in the human cerebral cortex. Brain Res 514:249–258.
Schwartz JH (1991) Synaptic vesicles. In: Principles of neural science (Kandel ER, Schwartz JH, Jessell TM, eds), pp 225–235. New York: Elsevier.
Seldon HL (1981a) Structure of human auditory cortex. I. Cytoarchitectonics and dendritic distributions. Brain Res 229:277–294.
Seldon HL (1981b) Structure of human auditory cortex. II. Axon distributions and morphological correlates of speech perception. Brain Res 229:295–310.
Seldon HL (1982) Structure of human auditory cortex. III. Statistical analysis of dendritic trees. Brain Res 249:211–221.
Seltzer B, Pandya DN (1989) Intrinsic connections and architectonics of the superior temporal sulcus in the rhesus monkey. J Comp Neurol 290:451–471.
Silver A (1974) The biology of cholinesterase. New York: Elsevier.
Small DH (1989) Acetylcholinesterases: zymogens of neuropeptide processing enzymes. Neuroscience 29:241–249.
Small DH (1990) Non-cholinergic actions of acetylcholinesterases: proteases regulating cell growth and development? Trends Biochem Science 15:213–216.
Strauss E, LaPointe JS, Wada JA, Gaddes W, Kosaka B (1985) Language dominance: correlation of radiological and functional data. Neuropsychologia 23:415–420.

Tago H, Kimura H, Maeda T (1986) Visualization of detailed acetylcholinesterase fiber and neuron staining in rat brain by a sensitive histochemical procedure. J Histochem Cytochem 34:1431–1438.
Taylor P, Schumacher M, MacPhee-Quigley K, Friedman T, Taylor S (1987) The structure of acetylcholinesterase: relationship to its function and cellular disposition. Trends Neurosci 10:93–95.
Terry RD, DeTeresa R, Hansen LA (1987) Neocortical cell counts in normal human adult aging. Ann Neurol 21:530–539.
von Economo C, Koskinas GN (1925) Die Cytoarchitektonik der Hirnrinde des erwachsenen Menschen. Berlin: Springer.
Witelson SF (1983) Bumps on the brain: right-left anatomic asymmetry as a key to functional asymmetry. In: Language functions and brain organization (Segalowitz S, ed), pp 117–143. New York: Academic.
Witelson SF, Kigar DL (1988) Asymmetry in brain function follows asymmetry in anatomical form: gross, microscopic, postmortem and imaging studies. In Handbook of neuropsychology (Boller F, Grafman J, eds), pp 111–142. New York: Elsevier
Zatorre RJ (1992) Lateralization of phonetic and pitch discrimination in speech processing. Science 256:846–849.